Electronic Supplementary Information (ESI)

Thioflavin-T Excimers Formation upon interaction with Amyloid Fibers

Raimon Sabate,*[a] Luis Rodriguez-Santiago ,[b] Mariona Sodupe,[b] Sven J Saupe,[c] and Salvador Ventura[d]

Sample preparation. Thioflavin-T (Th-T), insulin and all organic solvents were obtained from Sigma-Aldrich (St. Louis, MO, USA). Before use, Th-T was recrystallized three times in ethanol. The purity was verified by MALDI Mass spectroscopy. Th-T concentration nm in double-distilled water purified through a Milli-Q system (Millipore, USA) was determined using an absorptivity of 35 000 $M^{-1}\cdot cm^{-1}$ at 412 nm. Amylin Wt (and its Retro and Design forms), amyloid β peptide 1-40 (Aβ40) and 1-42 (Aβ42) were obtained from BioPeptide (San Diego, Ca, USA). HET-s(218-289), Sup35 and Ure2p proteins were expressed as a C-terminal histidine-tagged construct in *Escherichia coli* and purified under denaturing conditions (50 mMTris at pH 7.2, 300 mMNaCl and 6 M GuHCl buffer) for HET-s(218-289) and Sup35, and under native conditions (50 mMTris at pH 7.2, 300 mMNaCl buffer) for Ure2p by affinity chromatography on Talon histidine-tag resin (ClonTech, Mountain View, CA, USA). When necessary, buffer was exchanged by gel filtration on Sephadex G-25 column (Amersham, Uppsala, Sweden). The proteins were conserved at 277.15 K. For expression, 2 L DYT medium were inoculated with an overnight culture of BL21(DE3) bearing the plasmid to be expressed at 310.15 K. When an absorptivity at 600 nm of 0.8-1.0 was reached, the bacteria were induced with 1 mM of isopropyl-1-thio-β-D-galactopyranoside for 2 h at 310.15 K, then the culture was centrifuged and the cell pellet frozen at 253.15 K.Th-T bindings were performed at pH7 with a Th-T concentration of 25μM and 10 or 100μM of protein.

Methods. Gas phase geometry optimizations for Th-T have been carried out at the B3LYP[1-3] level of theory with the 6-31G(d) basis set. In the case of Th-T interacting with a model of the β-sheet structure, optimizations have been performed at the B3LYP-D level; that is, adding an empirical correction for dispersion of the form $-C_6\cdot R^{-6}$ (s_6=1.05)[4] to the B3LYP energy. In this case, we also used the 6-31G(d) basis set for geometry optimizations. The absorption spectra were computed using the TD-DFT methodology with the same functional and the 6-31++G(d,p) basis set by means of single point calculations at the optimized B3LYP/6-31G(d) geometries.

The absorption spectra of the dimer species were computed using the following procedure. Two Th-T molecules were placed aligned as shown in Figure S0 at a distance *d*. The distance *d* was kept fixed at 16, 17 and 18 Å. For each value of the distance *d* the value of α was varied from 180 to 75 degrees and the rest of the geometrical parameters were optimized at the B3LYP/6-31G(d) level. Finally, the absorption spectra were obtained by single point TD-DFT calculations at the optimized geometries using the B3LYP/6-31++G(d,p) method. All calculations were carried out with the Gaussian09 program package. [5]

Table 1 Th-T emission and excitation wavelengths in the presence of amyloid proteins and organic solvents

		λ^{ex}_{peak1}	λ^{ex}_{peak2}	λ^{ex}_{peak3}	λ^{ex}_{max}	λ^{em}_{max}
Organic solvent	Water	413.1	—	—	413.1	484.1
	EtOU	412.9	—	—	412.9	481.1
	Glycerol	418.0	—	—	418.0	485.6
	EG	416.8	—	—	416.8	486.0
	PEG	416.5	—	—	416.5	486.6
Amyloid proteins	Aβ40	418.7	434.9	441.1	436.9	480.0
	$A\beta42^{fib}$	417.7	434.0	441.7	438.9	480.0
	$Insulin^{mon}$	417.7	—	—	417.7	477.3
	$Insulin^{fib}$	420.2	431.9	442.4	430.0	480.7
	20-Residue amylin IAPP[a]					
	Wt^{fib}	421.5	437.9	450.1	443.6	480.0
	$Retro^{fib}$	419.7	432.4	448.1	444.1	478.1
	$Design^{fib}$	418.0	434.4	447.2	443.1	482.0
Prion proteins	$Sup35^{fib}$	417.2	434.3	449.3	445.1	481.3
	$Ure2p^{fib}$	418.4	433.1	446.4	438.7	479.1
	HET-s PFD[b]					
	pH 2^{mon}	412.9	—	—	412.9	482.6
	pH $2^{t\text{-}tib}$	419.1	431.4	442.9	441.1	481.5
	pH $5^{u\text{-}tib}$	418.9	430.6	445.3	442.9	479.1
	pH $7^{b\text{-}tib}$	421.3	435.5	445.8	435.2	481.3
	pH $7^{d\text{-}tib}$	421.2	433.0	442.3	422.3	481.4

[a] Amyloid fibrils formed by a 20-residue domain of the islet amyloid polypeptide (WT), as well as of a backward (RETRO) and scrambled (DESIGN) version of this peptide as reported in ref. 18. [b] Monomers and fibrillar variants formed under different conditions of HET-s PFD corresponding to the prion forming domain region (218–289) as reported in ref. 16. Note: λ^{ex} and λ^{em} are expressed in nm, and super-index mon, fib, t-fib, u-fib, b-fib and d-fib denote the terms: monomer, fibril, twisted-fibers, unitary-fibrils, bundled-fibrils and disordered-fibrils, respectively.

Table S2 Theoretical results gas phase Th-T and Th-T interacting with a model of a □-sheet structure

System	□[a]	□[ex]	f[b]
Th-T	34.1	403.5	0.856
Th-T···□-sheet	20.8	414.8	0.862

[a]Dihedral angle between the benzothiazole and the dimethylaniline moieties in the optimized ground state.

[b]Oscillator strength.

Table S3 Values of the wavelength for the two exciton-coupled states of the Th-T dimer computed at different distances and angles as defined in the methods section

	d=16 Å			**d=17 Å**			**d=18 Å**		
angle(□)	□$_1$	□$_2$	□□	□$_1$	□$_2$	□□	□$_1$	□$_2$	□□
180º	--	--	--	407.5	397.1	10.4	407.5	397.9	9.6
165º	408.5	396.4	12.1	407.8	397.3	10.5	407.2	398.2	9.0
150º	408.3	396.4	11.9	407.9	397.1	10.8	407.1	398.1	9.0
135º	408.2	396.4	11.8	407.9	397.0	10.9	407.1	397.7	9.4
120º	409.2	395.5	13.7	409.1	397.0	12.1	407.3	397.5	9.8
105º	410.8	396.3	14.5	409.9	397.0	12.9	408.7	396.9	11.8
90º	412.0	396.4	15.6	410.4	396.9	13.5	408.6	396.9	11.7
75º	411.3	394.7	16.6	410.2	395.8	14.4	409.7	396.6	13.1

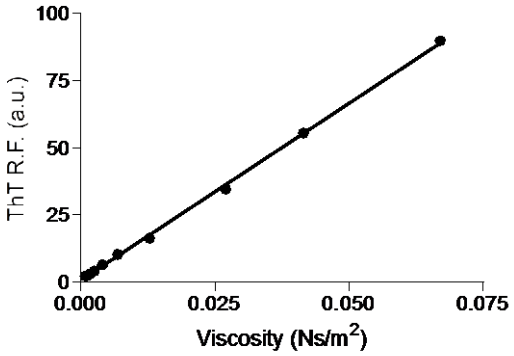

Fig. S1 Solvent viscosity dependence on Th-T fluorescence enhancement.

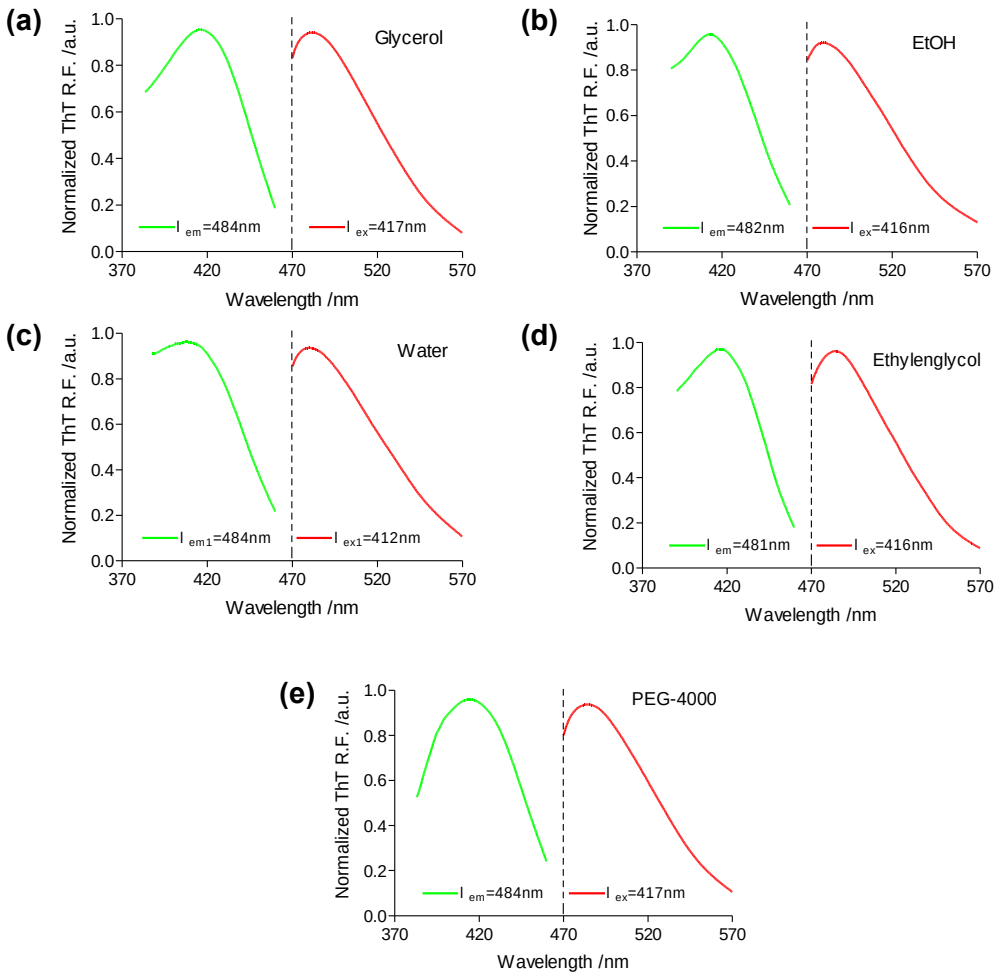

Fig. S2 Th-T normalized excitation and emission spectra in glycerol **(a)**, ethanol **(b)**, water **(c)**, ethylenglycol **(d)** and polyethylenglycol (PEG-4000) **(e)**.

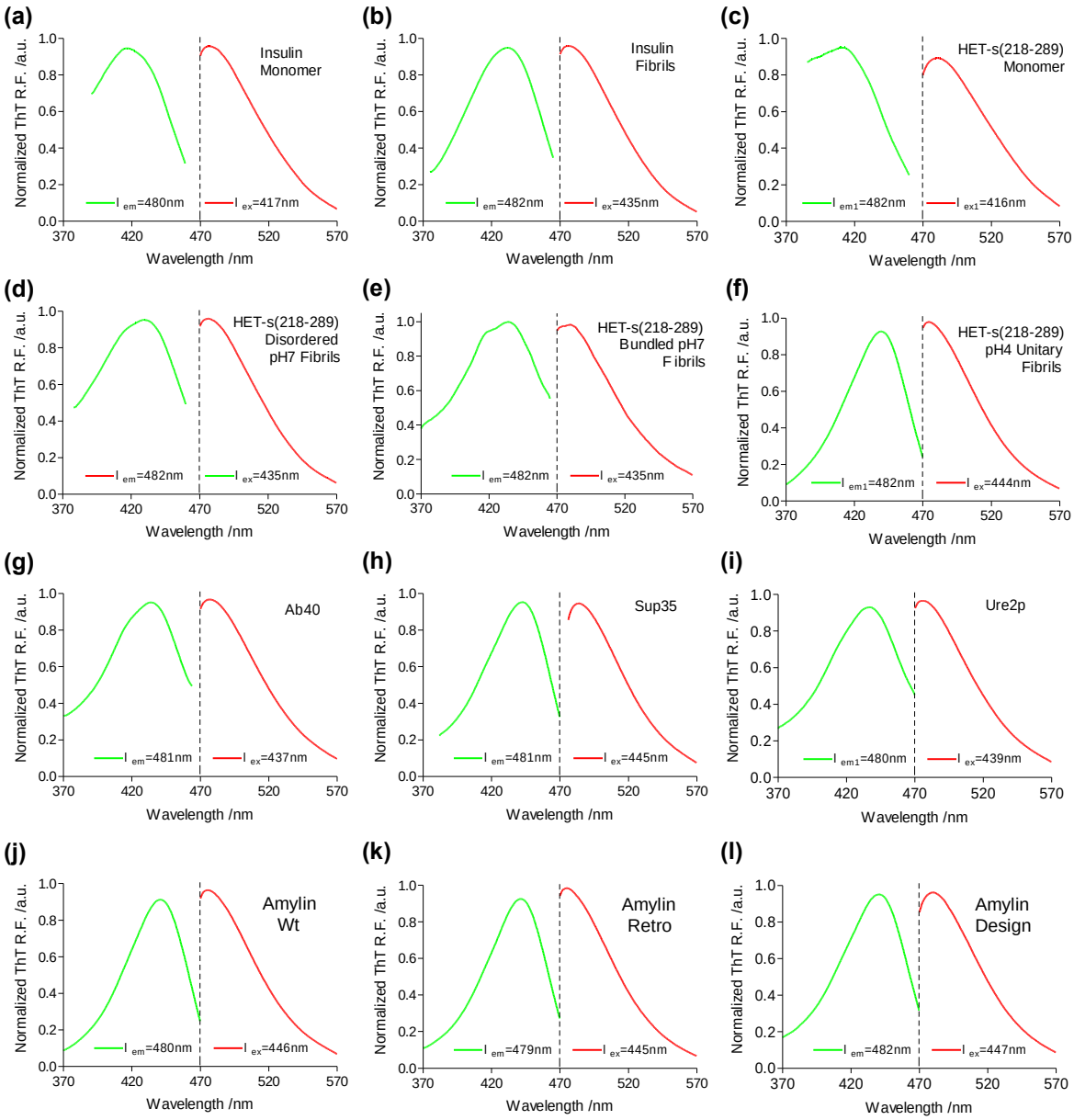

Fig. S3 Th-T excitation and emission spectra in presence of 100μM of soluble **(a)**and aggregated **(b)**insulin, and soluble **(c)** and disordered **(d)**, bundled **(e)**, unitary HET-s PFD fibrils**(f)**, and fibers of Aβ40 **(g)**, Sup35 **(h)**, Ure2p **(i)**, and amylin Wt**(j)**, Retro **(k)** and Design **(l)**.

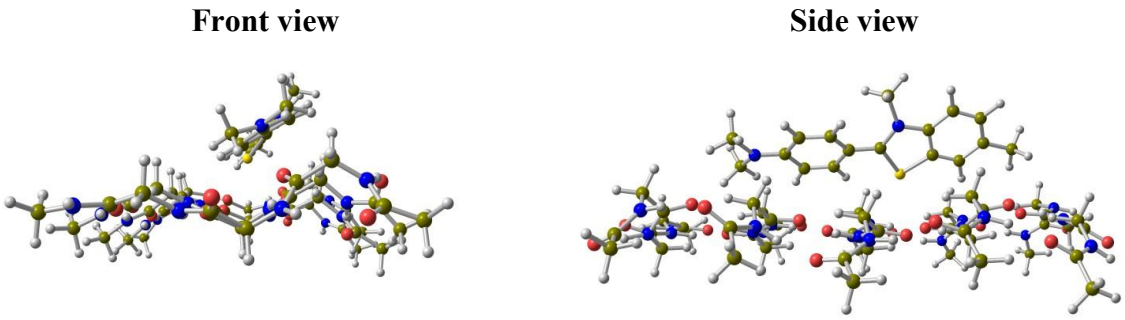

Fig. S4 B3LYP optimized structure of Th-T interacting with a model of a □-sheet made of five strands of the $CH_3(NHCOCH_2)_3NHCOCH_3$.

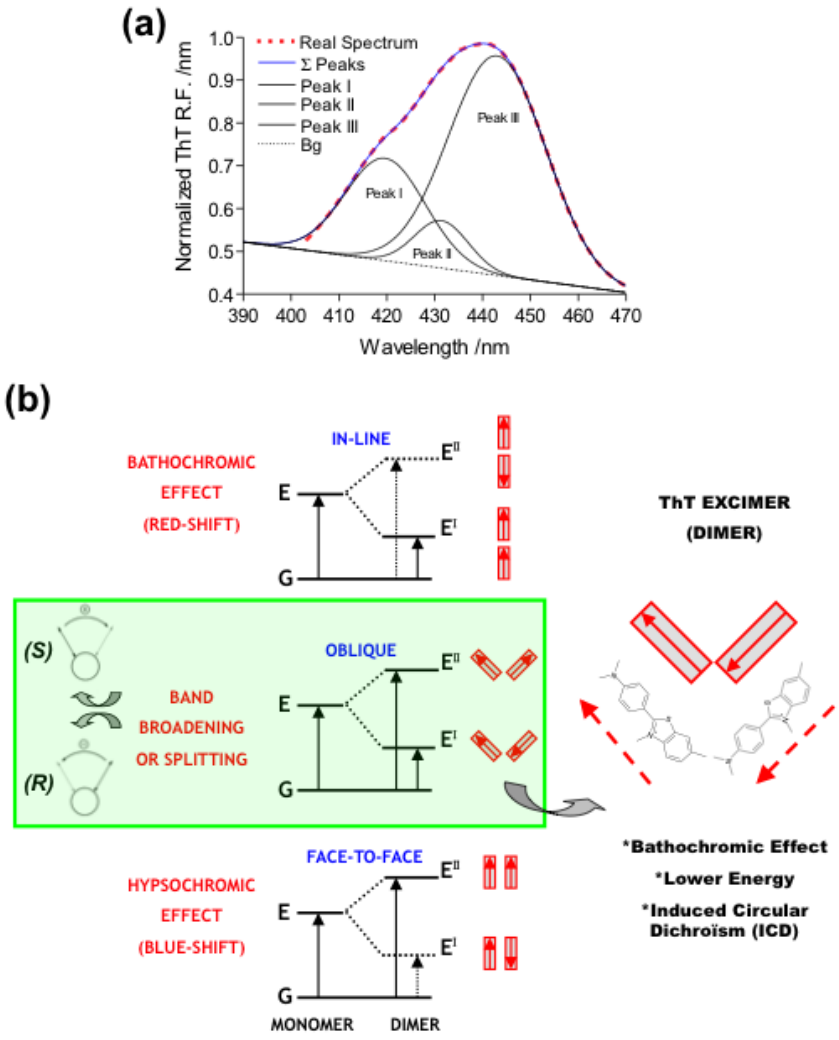

Fig. S5 Deconvolution of Th-T excitation spectrum in presence of amyloid fibrils **(a)** and scheme of Th-T dimer orientation options **(b)**. In the deconvolution, real spectra, ∑ peaks, peak I, II and III, and Bg are the Th-T excitation spectrum in presence of fibrils, the sum of deconvoluted peaks, each deconvoluted band and the baseline line, respectively The scheme displays the orientation dependence in exciton coupling between two Th-T monomers and their induced electric dipoles (double head arrows). The solid arrows connecting ground (G) and exited (E) states represent allowed transitions; the dashed arrows represent forbidden transitions. In-line (*J*-aggregate), oblique aggregate and face-to-face (*H*-aggregate) representation. Note that figure S5b is reprinted with permission from Ref. [19] in the main text.

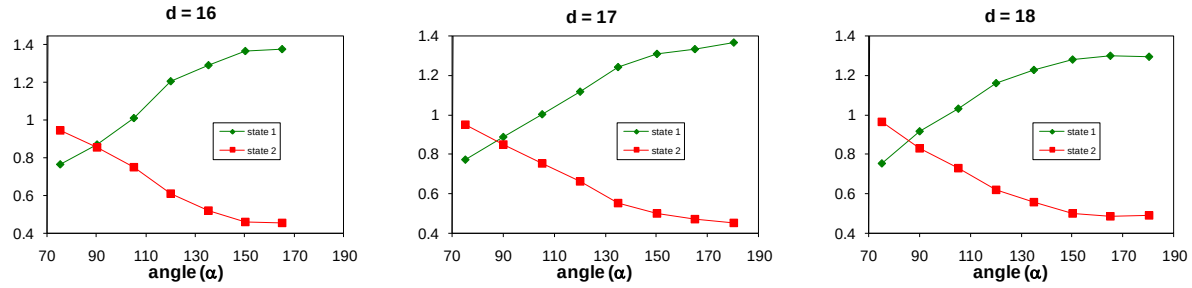

Fig. S6 Values of the oscillator strength for the two exciton-coupled states of the Th-T dimer computed at different distances and angles as defined in the methods section. Values of *d* are in Å and angles in degrees.

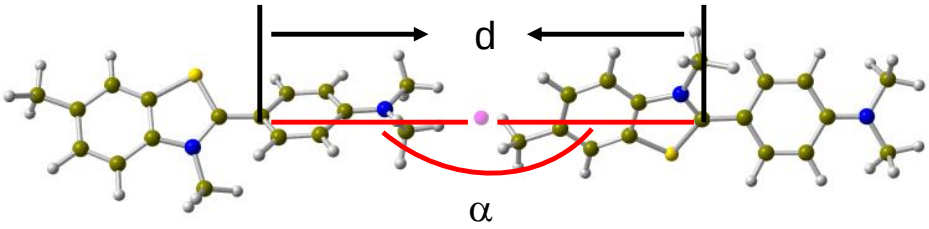

Figure S7. Parameters used to define the Th-T dimers.

References

1 A. D. Becke, *J. Chem. Phys.*, 1993, **98**, 5648.
2 C. Lee, W. Yang and R. G. Parr, *Phys. Rev. B.*, 1988, **37**, 785.
3 P. J. Stephens, F. J. Devlin, C. F. Chabalowski and M. J. Frisch, *Journal of Physical Chemistry*, 1994, **98**, 11623-11627.

4 S. Grimme, *Journal of Computational Chemistry*, 2006, **27**, 1787-1799.

5 M. J. T. Frisch, G. W.; Schlegel, H. B.; Scuseria, G. E.; Robb, M. A.; Cheeseman, J. R.; Scalmani, G.; Barone, V.; Mennucci, B.; Petersson, G. A.; Nakatsuji, H.; Caricato, M.; Li, X.; Hratchian, H. P.; Izmaylov, A. F.; Bloino, J.; Zheng, G.; Sonnenberg, J. L.; Hada, M.; Ehara, M.; Toyota, K.; Fukuda, R.; Hasegawa, J.; Ishida, M.; Nakajima, T.; Honda, Y.; Kitao, O.; Nakai, H.; Vreven, T.; Montgomery, Jr., J. A.; Peralta, J. E.; Ogliaro, F.; Bearpark, M.; Heyd, J. J.; Brothers, E.; Kudin, K. N.; Staroverov, V. N.; Kobayashi, R.; Normand, J.; Raghavachari, K.; Rendell, A.; Burant, J. C.; Iyengar, S. S.; Tomasi, J.; Cossi, M.; Rega, N.; Millam, N. J.; Klene, M.; Knox, J. E.; Cross, J. B.; Bakken, V.; Adamo, C.; Jaramillo, J.; Gomperts, R. E.; Stratmann, O.; Yazyev, A. J.; Austin, R.; Cammi, C.; Pomelli, J. W.; Ochterski, R.; Martin, R. L.; Morokuma, K.; Zakrzewski, V. G.; Voth, G. A.; Salvador, P.; Dannenberg, J. J.; Dapprich, S.; Daniels, A. D.; Farkas, O.; Foresman, J. B.; Ortiz, J. V.; Cioslowski, J.; Fox, D. J., in *Gaussian 09, revision C.01*, ed. I. Gaussian, Wallingford, CT,, 2009.